CHEMISTRY
A European Journal

A Journal of
ChemPubSoc Europe

Accepted Article

Title: A water-soluble, two-photon probe for imaging endogenous hypochlorous acid in live tissue

Authors: Panfei Xing, Yanxian Feng, Yiming Niu, Qiu Li, Zhe Zhang, Lei Dong, and Chunming Wang

To be cited as: *Chem. Eur. J.* 10.1002/chem.201800249

Link to VoR: http://dx.doi.org/10.1002/chem.201800249

Supported by
ACES

WILEY-VCH

10.1002/chem.201800249

WILEY-VCH

COMMUNICATION

A water-soluble, two-photon probe for imaging endogenous hypochlorous acid in live tissue

Panfei Xing,[a] Yanxian Feng,[a] Yiming Niu,[a] Qiu Li,[a] Zhe Zhang,[a] Lei Dong,*[b] and Chunming Wang*[a]

Abstract: Detection of hypochlorous acid (HClO) in the living system may help to uncover its essential biological functions. However, current imaging agents suffer from poor water solubility that limits their live-tissue applications. Here, we devised a water-soluble probe (**NNH**) by innovative hydrazone modification of 1,8-naphthalimide at 3' position, which was successfully applied to tracking endogenous HClO in both cultured macrophages and a liver injury model in mice. **NNH** demonstrated remarkably increased water solubility and multiple desirable features including two-photon absorbance, anti-bleaching capability, rapid cellular uptake, and low cytotoxicity. In summary, we report **NNH** as the first hydrazone-based probe for real-time imaging of HClO in live tissue.

Hypochlorous acid (HClO) is an important component of reactive oxygen species (ROS). In the living system, it is generated by the catalysis of myeloperoxidase (MPO) in the presence of chloride and hydrogen peroxide.[1] Increasing evidence suggests that HClO plays essential roles in various pathological changes, such as the development of atherosclerosis and rheumatoid arthritis;[2] however, to uncover more of its mechanisms in these processes, a sensitive, non-invasive and real-time detection tool is in pressing demand. Among the different types of tools, fluorescent probes with two-photon absorbance are particularly attractive, as they not only meet the above requirements, but also have such advantages as deep tissue penetration and reduced background noise.[3] Nevertheless, most existing two-photon probes for HClO imaging are poorly soluble in water, and require additional solvent when used.[4] Design of a water-soluble dye for HClO imaging, with two-photon absorbance and other favorable features, can lead to safer and broader application of such probes in the living system.

Selection of a fluorophore with adequate brightness and photo stability is crucial for the development of such a probe.[5] Recent studies demonstrated 1,8-naphthalimide-based fluorescent probes with excellent optical properties, including high quantum yields, a large stokes shift, and photo stability.[6] Importantly, 1,8-naphthalimide derivatives have two-photon absorbance.[7] Its structure is also desirable for probes design. First, its core unit is a rigid planarity naphthalene ring, which is structurally stable. Second, its 1' and 8' positions are electron acceptors, and 4' site is an electron donor, offering an inducible intramolecular charge transfer (ICT) mechanism. Normally, these probes are prepared by replacing hydroxyl (-OH) or amine (-NH_2) at the 4' position of 1,8-naphthalimide derivatives with functional groups, constructing an ICT system that enable the probe to work. But these compounds are highly hydrophobic and poorly water-soluble.[8] One example compound synthesized based on this strategy for HClO imaging is O-(N-butyl-1,8-naphthalimide)-4-yl-N,N-dimethylthiocarbamate (**NDMTC**). The introduction of N,N-dimethylthiocarbamate (DMTC) onto N-butyl-4-hydroxy-1,8-naphthalimide resulted in the quenched fluorescence, attributing to the highly effective inhibition of ICT effect. However, due to its poor solubility, this probe was dissolved in a PBS/ethanol (1:1, v/v, pH 7.4) buffer solution for use.[4c]

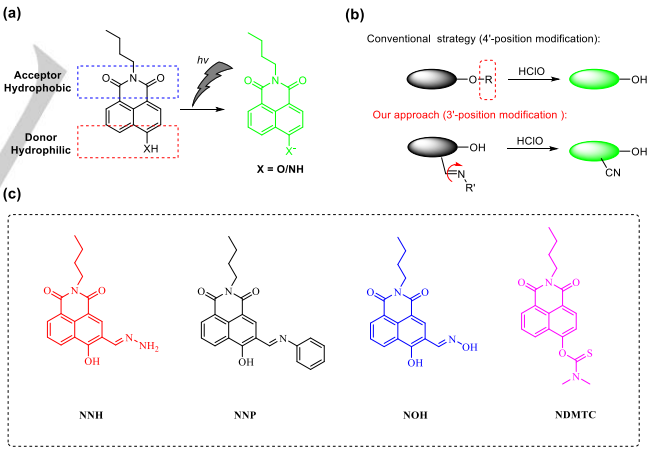

Scheme 1 Design and synthesis of probes for HClO. (a) General structure of 1,8-naphthalimide derivatives; (b) Conventional (4'-position modification) and our strategy (3'-position modification) for designing HClO probes; (c) The structures of products based on our approach (**NNH**, **NNP**, **NOH)** and the conventional approach (**NDMTC**).

We hypothesized that modification of a C=N to the 3' position of 1,8-naphthalimide derivatives could generate a probe with all desirable optical features but significantly increased hydrophilicity. Our hypothesis was based on two considerations. First, N-butyl-4-hydroxy-1,8-naphthalimide has a rigid structure, making 3' position the only modifiable site. Thus, the formylated product N-

[a] P. Xing, Y. Feng, Y. Niu, Q. Li, Z. Zhang, C. Wang
State Key Laboratory of Quality Research in Chinese Medicine, Institute of Chinese Medical Sciences, University of Macau
Avenida da Universidade, Macau SAR, China
E-mail: CMWang@umac.mo
[b] L. Dong
State Key Laboratory of Pharmaceutical Biotechnology, Nanjing University Institution
Nanjing, 210093, China
E-mail: leidong@nju.edu.cn

Supporting information for this article is given via a link at the end of the document.

10.1002/chem.201800249

butyl-4-hydroxy-3-aldehyde-1,8-naphthalimide can be easily obtained through the Duff reaction – while preserving the hydrophilic -OH at 4' position. Second, to achieve an off-on fluorescent response, we focused on the formation of C=N double bond, which can be isomerized and decay the energy of the compounds in the excitation state, leading to quenching of the fluorescence. When the rotation is restricted or C=N removed, the compounds can release fluorescence.[9] Generally, C=N bond can be an oxime (-C=N-OH) or a hydrazone moiety (-C=N-NH_2). As illustrated in Scheme 1c, we started with the commercially available 4-bromo-1,8-naphthalic anhydride to obtain N-butyl-4-hydroxy-3-aldehyde-1,8-naphthalimide in a simple synthetic process, and continued to fabricate **NNH**, **NOH**, and **NNP** based on the aldehyde product. Meanwhile, we prepared **NDMTC** as a control compound representing the 4' position modification.

Our data demonstrated that two derivatives based on 3'-position modification, **NNH** and **NOH**, had significantly increased water solubility, compared with the fluorophore core and the control compound **NDMTC**. First, the mean contact angle of the water droplets on glass coated with **NNH** and **NOH** was 39.8° and 44.4°, respectively, markedly lower than 93.8° of that on **NDMTC** (Figure 1a). Interestingly, even though having a phenyl group at its 3' position, the compound **NNP** (80.1°) is still more hydrophilic than **NDMTC**, in agreement with our assumption. Next, ultraviolet spectrophotometry revealed that the mean maximum concentration of **NNH** and **NOH** in PBS solution (10 mM, pH 7.4) was 302 and 200 μM, respectively, while **NDMTC** precipitated (Figure 1b). In addition, a group of high frame rate videos showed that **NDMTC** (5 mM in DMSO, 6 μL) immediately precipitated when added into PBS (10 mM, pH 7.4, 3 mL; Figure 1c) but dissolved better in PBS/EtOH (1/1, v/v, 3 mL; Figure 1d). In contrast, **NOH** exhibited higher water solubility in PBS (10 mM, pH 7.4; Figure 1e). These results confirmed that the modification at the 3' position of the 1,8-naphthalimide core effectively increased the water solubility, compared with the conventionally performed 4'-modification. As designed, the hydroxyl or amino group at the terminal of C=N bond could substantially improve the hydrophilicity of the compound.

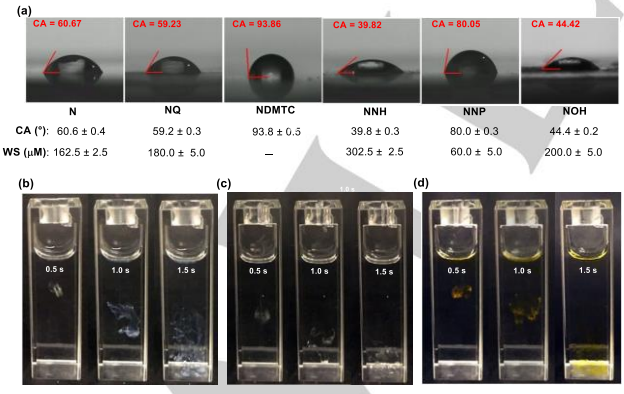

Figure 1 Evaluation of the water solubility of the compounds. (a) Contact angles of water on the glass surface for **N**, **NQ**, **NDMTC**, **NNH**, **NOH**, and **NNP**; (b) Solubility and contact angel values of **N**; **NQ**, **NDMTC**, **NNH**, **NOH**, and **NNP**; (c-e) screenshot of videos at 0.5, 1.0, and 1.5 s showing (c) **NDMTC** in PBS (10 mM, pH 7.4), (d) **NDMTC** in PBS/EtOH (1/1, v/v), and (e) **NOH** in PBS (10 mM, pH 7.4).

To study the capability of **NNH**, **NOH** and **NDMTC** in detecting HClO, we measured the photophysical properties in absolute PBS (10 mM, pH 7.4). As expected, the C=N bond on **NNH** (-C=N-NH_2) or **NOH** (-C=N-OH) led to almost non-fluorescence emission. With the addition of HClO, the florescence intensity increased significantly, resulted from the oxidation breaking of the hydrazone or oxime by HClO (Figure 2a and 2b). We next prepared HClO in different concentrations to study the sensitivity of **NNH** (in the range of 0-190 μM) and **NOH** (in the range of 0-210 μM). Both dyes showed a linear standard calibration curve, plotted between the fluorescence intensity (emission 525 nm) and concentration of HClO (Figure S3), with a correlation coefficient of 0.998 and 0.995, respectively. The limit of detection (LOD) for **NNH** and **NOH** was 29.3 nM and 87.4 nM, respectively, showing a high sensitivity compared with reported work.[10] In contrast, **NDMTC** (10 μM) emitted no fluorescence in response to HClO (100 μM) in PBS (10 mM, pH 7.4), but did so when the solution was changed to a mixture of PBS (10 mM, pH 7.4) and ethyl alcohol (EtOH) and generated higher fluorescent intensity in solution with a higher EtOH percentage (Figure 2d). These findings indicated that poor hydrophilicity was a key obstacle for **NDMTC** in detecting HClO, which underpinned our motivation of improving the water solubility of the dye.

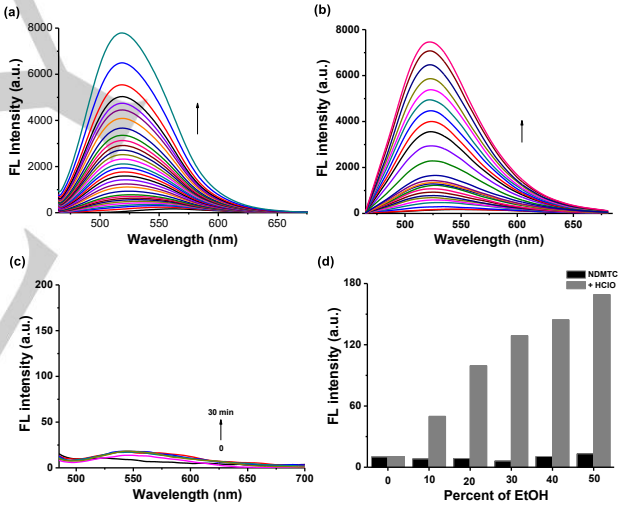

Figure 2 Photophysical properties of **NNH**, **NOH**, and **NDMTC**. (a) Fluorescence titration of **NNH** (5 μM) towards HClO (0-190 μM) in PBS (10 mM, pH 7.4); (b) Fluorescence titration of **NOH** (5 μM) towards HClO (0-210 μM) in PBS (10 mM, pH 7.4); (c) Time dependent (0-30 mins) fluorescent spectrum of **NDMTC** (10 μM) with the addition of HClO (100 μM) in PBS (10 mM, pH 7.4); (d) Fluorescence intensity changes of **NDMTC** (10 μM) with the addition of HClO (100 μM) in PBS (10 mM, pH 7.4, containing different percent of EtOH).

To assess their selectivity for HClO, we examined the response of **NNH** and **NOH** to a series of other ROS molecules: nitric oxide free radicals (NO·), peroxynitrite anion ($ONOO^-$), peroxy anion ($O_2^{\cdot-}$), nitrite anion (NO_2^-), hydrogen peroxide (H_2O_2), tert-butyl hydroperoxide (*t*BuOOH), and hydroxyl radical (·OH). As shown in Figure S4, these two probes generated remarkably higher fluorescent intensity in response to HClO than to other molecules, confirming its highly selective detection of HClO is not disrupted

10.1002/chem.201800249

by other ROS/RNS when they are present in comparable concentrations.

We next investigated the mechanism of **NNH** and **NOH** towards HClO, by acquiring the HRMS spectra of these two probes with the addition of HClO. The spectra showed that (Figure S25) the addition of HClO triggered a peak at m/z 317.0905, which could be attributed to the structure of N-butyl-4-hydroxy-3-cyano-1,8-naphthalimide (calculated value: 317.0902, $[M+Na]^+$). For **NOH**, the addition of HClO triggered a peak of $[M-H]^-$ (Figure S26). The result indicated the oxidative cleavage of hydrazone moiety or oxime moiety by HClO, in agreement with the conclusion drawn from the fluorescent spectra.

Cell toxicity and uptake efficiency are two crucial parameters for a probe to be applied into the living system. We first evaluated the toxicity of **NNH** and **NOH** to RAW 264.7 cells with MTT assay. After a 24-h incubation, **NNH** and **NOH** in a range of concentrations (5-30 μM) exerted no adverse effect to the cells (viability > 90%, Figure S7). We further tested the cellular uptake efficiency of the two probes, pretreating the cells with HClO (20 μM) and adding either probe (5 μM) into the culture. Intriguingly, the two probes showed distinct uptake kinetics – the uptake of **NNH** peaked at 10 min while that of **NOH** at 20 min (Figure 3b and S8). We speculated that this difference could be attributed to the different functional groups at the end of 3' position, which rendered **NNH** (pKa = 5.71) to appear positive and **NOH** (pKa = 9.83) negative under the physiological pH. The former might thus be more affinitive to the cells with an overall negative surface charge,[11] enabling a faster uptake of **NNH** than **NOH**.

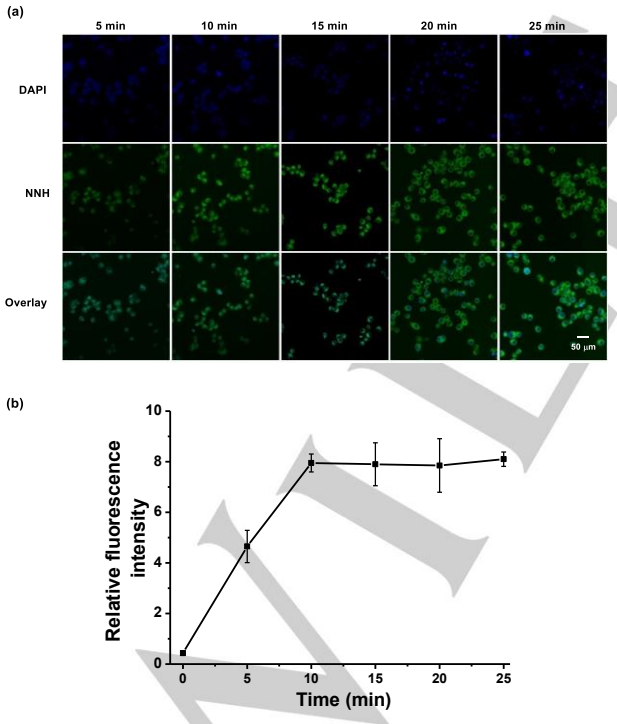

Figure 3 Cellular uptake of **NNH**. Confocal images of RAW 264.7 cells co-stained with 5 μM **NNH** and DAPI (100 ng mL^{-1}) in different incubation time. Cells were pretreated with 20 μM NaClO. The excitation wavelength for one-photon imaging was 445 nm and the emissions were collected at 430-460 nm for DAPI and 480–550 nm, respectively for **NNH**. Scale bar was 50 μm.

Based on the above findings, we selected **NNH** as the representative probe based on 3'-position modification of 1,8-naphthalimide, and evaluated its performance in tracking endogenous HClO in living cells and tissue. First, we incubated murine macrophage cell line (RAW 264.7) with **NNH** (5 μM) and DAPI (100 ng mL^{-1}). The cells received – i) no further treatment (control group); ii) NaClO (20 μM) to generate exogenous HClO; or iii) lipopolysaccharide (LPS, 0.5 μg mL^{-1}) plus phorbolmyristate acetate (PMA, 1 μg mL^{-1}) as an established protocol to induce endogenous HClO.[12] We observed that **NNH** generated barely any fluorescence in the control group but strong fluorescence in the HClO-treated cells (Figure 4b and c) – and this fluorescent intensity increased as the concentration of NaClO rose within the range of 0-20 μM (Figure 4d). In addition to exogenous HClO, **NNH** also responded to endogenously produced HClO, by exhibiting green fluorescence in the third group of cells (Figure 4b) and its intensity was comparable to that in the second group (Figure 4c). According to our calculation, the concentration of endogenous HClO triggered under this condition should fall into the range of 15-20 μM. Taken together, these data demonstrated that **NNH** could detect rapidly and sensitively to both exogenous and endogenous HClO intracellularly. However, **NDMTC**, representing the water-insoluble product of conventional 4'-position modification, failed to provide signals in any groups (Figure 4a). This result was consistent with the previous findings on photophysical properties, and further highlighted how important the water solubility of the probes was for their application potential in biological samples.

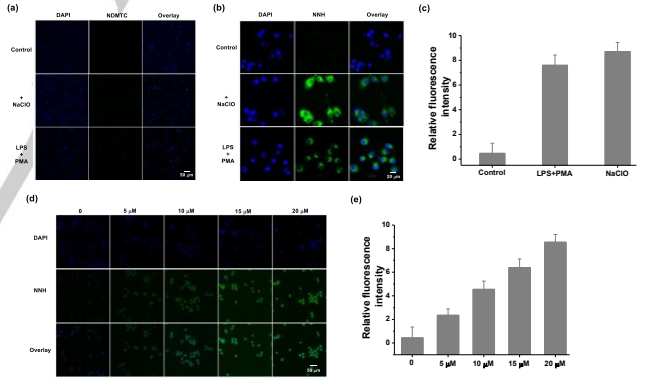

Figure 4 One-photon imaging of exogenous and endogenous HClO. (a) and (b) RAW 264.7 cells were incubated with HClO (20 μM) for 20 min or stimulated with LPS (0.5 μg mL^{-1})/PMA (1 μg mL^{-1}) for 24 h. Then one-photon images of RAW 264.7 cells co-stained with 20 μM **NDMTC** for 20 min and DAPI (100 ng mL^{-1}) for another 10 min by confocal for (a). Scale bar was 50 μm; One-photon images of RAW 264.7 cells co-stained with 5 μM **NNH** for 10 min and DAPI (100 ng mL^{-1}) for another 10 min by confocal for (b). Scale bar was 20 μm; (d) RAW 264.7 cells were incubated with different concentration of HClO (0-20 μM) for 20 min. Then one-photon images of RAW 264.7 cells co-stained with 5 μM **NNH** for 10 min and DAPI (100 ng mL^{-1}) for another 10 min by confocal. Scale bar was 50 μm. The excitation wavelength for **NNH** was 445 nm and the emissions were collected at 480–550 nm; The excitation wavelength for **NDMTC** was 488 nm and the emissions were collected at 520-580 nm; The excitation wavelength for DAPI was 405 nm and the emissions were collected at 430-460 nm.

It is well known that probes with two-photon absorbance have advantages such as reduced background signal.[13] This was also the reason we chose a two-photon fluorophore as the basis of our

design. To confirm that **NNH** (and also **NOH**) preserved this key feature, we examined the performance of these probes in detecting endogenous and exogenous HClO with a two-photon microscopy, using the same experimental conditions as in the one-photon imaging). As shown in Figure S8, under the excitation at 800 nm, both **NNH**- and **NOH**-labeled cells showed no signals until the addition of NaClO or LPS+PMA, which triggered bright green fluorescence after a 20-min incubation. Clearly, **NNH** possessed the desirable two-photon absorbance feature in the imaging of exogenous and endogenous HClO in the cultured macrophages.

We finally examined the efficacy of **NNH** in imaging HClO in the live tissue in a CCl_4-induced liver injury model. Liver injury is a common clinical issue related to a wide range of diseases; but it is difficult to predict in practice.[14] One most established model of liver injury was induced by CCl_4 in mice, in which CCl_4 can be metabolized by P450 in the hepatocytes to produce abundant ROS, leading to severe oxidative liver injury.[15] So, it would be interesting if **NNH** could track the production of HClO in this model, which might further provide useful information. We generated this model by intraperitoneal injection of 6-8 weeks mice with CCl_4 (50%, in olive oil).[16] After 24 h, we isolated liver tissues and injected **NNH** (20 μL, 5 mM) or **NDMTC** (20 μL, 5 mM, as control probe), and confirmed the successful establishment of liver injury in the two treatment groups by determination of MPO activity (Figure 5b). Then, we observed that the group injected with **NNH** showed strong fluorescence while that with **NDMTC** emitted no signal (Figure 5a). This result suggested that **NNH** was capable of detecting endogenous HClO in the zone with liver injury, but, again, the conventional, water-insoluble product of **NDMTC** was incapable to do so.

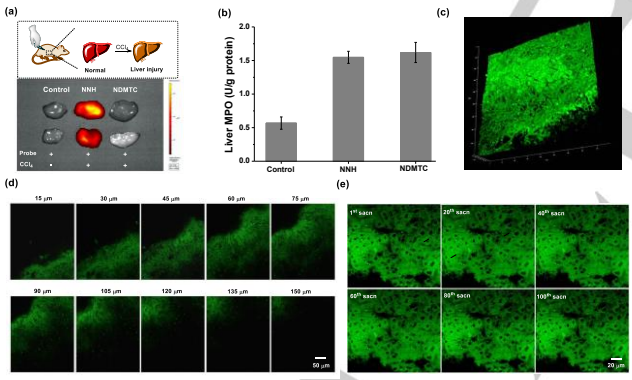

Figure 5 Two-photon imaging of HClO in CCl_4-induced liver injury model of mice. (a) Diagram of CCl_4-induced liver injury in mice and liver tissue fluorescence images with **NNH** and **NDMTC**; (b) MPO activity assay of CCl_4-induced liver injury model; (c) 3D mapping of CCl_4-induced liver tissue under 800 nm excitation; (d) Depth scan (15-150 μm) in the CCl_4-induced liver tissue under 800 nm excitation. Scale bar was 50 μm; (e) Photostability of **NNH** acquired under continuous excitation (800 nm). Scale bar was 20 μm

We noticed two remarkable features of **NNH** in this live-tissue imaging. First, its two-photon fluorescence enabled us to observe clear fluorescent signals at different horizontal plane of a complete liver – without the need of slicing. Under two-photon excitation (800 nm), the penetration reached as deep as 150 μm (Figure 5c and d). Second, **NNH** demonstrated notable photostability against photo-bleaching throughout our experiment. To quantitatively evaluate this, we performed a continuous scanning of the **NNH**-labeled liver slices under laser irradiation. Only 3% of the fluorescence lost after 100 scans, which highlighted the property of **NNH** in resisting photo-bleaching (Figure 5e and S10). These are perhaps the two most sought-after advantages, among many others, of a fluorescent probe designed for live tissue imaging.

In summary, we report the design of **NNH**, a water-soluble fluorescent probe for real-time tracking of HClO in live tissue and cells, with multiple desirable features including two-photon absorbance, anti-bleaching capability, efficient cellular uptake and no cytotoxicity. The key innovation in designing **NNH** is a radical, but simple, change in the position of chemical modification to a fluorophore. Compared with conventional approach to modify 1,8-naphthalimide derivatives at 4' position, we modified it at 3' position to introduce a hydrazone, thereby retaining the hydroxy group and the optical features of the compound – while substantially improving the water solubility of the product. Serial follow-up tests highlighted that this improvement was crucial for the performance of the probe in the living system. As the first hydrazone-based probe for similar purposes, **NNH** may serve as an imaging tool for uncovering the roles of HClO in broad pathological processes.

Acknowledgements

We thank funding supports from Science and Technology Development Fund, Macao SAR (FDCT 080/2016/A2, 126/2016/A3), University of Macau (MYRG2016-00031-ICMS-QRCM) and National Science Foundation of China (51503232).

Keywords: water-soluble • two-photon • fluorescent probe • endogenous hypochlorous acid • live tissue

[1] P. S. Hole, R. L. Darley, A. Tonks, *Blood* **2011**, *117*, 5816-5826.

[2] a) A. Daugherty, J. L. Dunn, D. L. Rateri, J. W. Heinecke, *J. Clin. Invest.* **1994**, *94*, 437; b) P. Wei, W. Yuan, F. Xue, W. Zhou, R. Li, D. Zhang, T. Yi, *Chem. Sci.* **2018**. *9*, 495-501.

[3] G. S. He, L.-S. Tan, Q. Zheng, P. N. Prasad, *Chem. Rev.* **2008**, *108*, 1245-1330; b) Q. Xu, C. Heo, G. Kim, H. Lee, H. Kim, J. Yoon, *Angew. Chem. Int. Edit.* **2015**, *54* 4890-4894; c) H. Kim, B. Cho, *Chem. Rev.* **2015**, *115*, 5014-5055.

[4] a) Y. Feng, S. Li, D. Li, Q. Wang, P. Ning, M. Chen, X. Tian, X. Wang, *Sens. Actuators B: Chem.* **2018**, *254*, 282-290; b) Q. Xu, C. H. Heo, J. A. Kim, H. S. Lee, Y. Hu, D. Kim, K. M. K. Swamy, G. Kim, S.-J. Nam, H. M. Kim, *Anal. Chem.* **2016**, *88*, 6615-6620; c) B. Zhu, P. Li, W. Shu, X. Wang, C. Liu, Y. Wang, Z. Wang, Y. Wang, B. Tang, *Anal. Chem.* **2016**, *88*, 12532-12538.

[5] X. Liu, Q. Qiao, W. Tian, W. Liu, J. Chen, M. J. Lang, Z. Xu, *J. Am. Chem. Soc.* **2016**, *138*, 6960-6963.

[6] a) Y. Tang, X. Kong, A. Xu, B. Dong, W. Lin, *Angew. Chem. Int. Edit.* **2016**, *55*, 3356-3359; b) X.-X. Zhang, H. Wu, P. Li, Z.-J. Qu, M.-Q. Tan, K.-L. Han, *Chem. Commun.* **2016**, *52*, 8283-8286; c) Y. Li, X. Xie, X. e. Yang, M. Li, X. Jiao, Y. Sun, X. Wang, B. Tang, *Chem. Sci.* **2017**, *8*, 4006-4011; d) Z.-R. Dai, L. Feng, Q. Jin, H. Cheng, Y. Li, J. Ning, Y. Yu, G.-B. Ge, J.-N. Cui, L. Yang, *Chem. Sci.* **2017**, *8*, 2795-2803; e) Y. Kim,

Y. Jang, S. Mulay, T. Nguyen, D. Churchill, *Chem-Eur. J.* 2017, **23**, 7785-7790.

[7] a) M. Ren, B. Deng, J.-Y. Wang, X. Kong, Z.-R. Liu, K. Zhou, L. He, W. Lin, *Biosens. Bioelectr.* **2016**, *79*, 237-243; b) Z.-R. Dai, G.-B. Ge, L. Feng, J. Ning, L.-H. Hu, Q. Jin, D.-D. Wang, X. Lv, T.-Y. Dou, J.-N. Cui, L. Yang, *J. Am. Chem. Soc.* **2015**, *137*, 14488-14495.

[8] a) M. Cao, H. Chen, D. Chen, Z. Xu, S. H. Liu, X. Chen, J. Yin, *Chem. Commun.* **2016**, *52*, 721-724; b) N. R. Chereddy, M. V. Niladri Raju, P. Nagaraju, V. R. Krishnaswamy, P. S. Korrapati, P. R. Bangal, V. J. Rao, *Analyst* **2014**, *139*, 6352-6356; c) M. H. Lee, N. Park, C. Yi, J. H. Han, J. H. Hong, K. P. Kim, D. H. Kang, J. L. Sessler, C. Kang, J. S. Kim, *J. Am. Chem. Soc.* **2014**, *136*, 14136-14142; d) Y. Tian, F. Xin, C. Gao, J. Jing, X. Zhang, *J. Mater. Chem. B* **2017**, *5*, 6890-6896.

[9] a) X. Cheng, H. Jia, T. Long, J. Feng, J. Qin, Z. Li, *Chem. Commun.* **2011**, *47*, 11978-11980; b) S.-Y. Yu, C.-Y. Hsu, W.-C. Chen, L.-F. Wei, S.-P. Wu, *Sens. Actuators B: Chem.* **2014**, *196*, 203-207; c) S. I. Reja, V. Bhalla, A. Sharma, G. Kaur, M. Kumar, *Chem. Commun.* **2014**, *50*, 11911-11914; d) W. Lin, L. Long, B. Chen, W. Tan, *Chem-Eur. J.* **2009**, *15*, 2305-2309.

[10] a) Y. W. Jun, S. Sarkar, S. Singha, Y. J. Reo, H. R. Kim, J.-J. Kim, Y.-T. Chang, K. H. Ahn, *Chem. Commun.* **2017**, *53*, 10800-10803; b) F. Tian, Y. Jia, Y. Zhang, W. Song, G. Zhao, Z. Qu, C. Li, Y. Chen, P. Li, *Biosens. Bioelectr.* **2016**, *86*, 68-74; c) B. Zhang, X. Yang, R. Zhang, Y. Liu, X. Ren, M. Xian, Y. Ye, Y. Zhao, *Anal. Chem.* **2017**, *89*, 10384-10390.

[11] M. P. Calatayud, B. Sanz, V. Raffa, C. Riggio, M. R. Ibarra, G. F. Goya, *Biomaterials* **2014**, *35*, 6389-6399.

[12] a) H. Xiao, K. Xin, H. Dou, G. Yin, Y. Quan, R. Wang, *Chem. Commun.* **2015**, *51*, 1442-1445; b) G. Li, Q. Lin, L. Sun, C. Feng, P. Zhang, B. Yu, Y. Chen, Y. Wen, H. Wang, L. Ji, H. Chao, *Biomaterials* **2015**, *53*, 285-295.

[13] Z. Mao, H. Jiang, Z. Li, C. Zhong, W. Zhang, Z. Liu, *Chem. Sci.* **2017**, *8*, 4533-4538.

[14] W. R. Proctor, A. J. Foster, J. Vogt, C. Summers, B. Middleton, M. A. Pilling, D. Shienson, M. Kijanska, S. Ströbel, J. M. Kelm, P. Morgan, S. Messner, D. Williams, *Arch. Toxicol.* **2017**, *91*, 2849-2863.

[15] L. W. Weber, M. Boll, A. Stampfl, *Crit. Rev. Toxicol.* **2003**, *33*, 105-136.

[16] J. Dai, M. Liu, Q. Ai, L. Lin, K. Wu, X. Deng, Y. Jing, M. Jia, J. Wan, L. Zhang, *Chem. Biol. Interact.* **2014**, *216*, 34-42.

10.1002/chem.201800249

WILEY-VCH

COMMUNICATION

Here, we devised a water-soluble probe (**NNH**) by innovative hydrazone modification of 1,8-naphthalimide at 3' position, which was successfully applied to tracking endogenous HClO in both cultured macrophages and a liver injury model in mice. **NNH** demonstrated remarkably increased water solubility and multiple desirable features including two-photon absorbance, anti-bleaching capability, rapid cellular uptake, and low cytotoxicity.

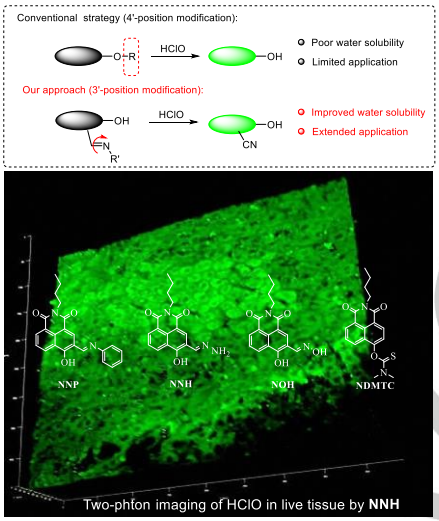

Panfei Xing,[a] Yanxian Feng,[a] Yiming Niu,[a] Qiu Li,[a] Zhe Zhang,[a] Lei Dong,[b] and Chunming Wang*[a]*

Page No. – Page No.
A water-soluble, two-photon probe for imaging endogenous hypochlorous acid in live tissue